JOURNAL OF AIRCRAFT
Vol. 48, No. 4, July–August 2011

Buckling Behavior of an Orthotropic Plate Strip Under Combined Compression and Shear

M. Beerhorst* and M. Seibel†
HAW Hamburg, 20099 Hamburg, Germany
and
C. Mittelstedt‡
ELAN GmbH, 21079 Hamburg, Germany

DOI: 10.2514/1.C031284

The present contribution deals with the buckling behavior of a theoretical, infinitely long plate. At the longitudinal edges, the plate strip is assumed to be elastically restrained against rotation, whereas no specific assumptions toward the boundary conditions at the transversal edges are made. A combination of homogeneous uniaxial compression in the longitudinal direction and in-plane shear is considered as loading condition. The homogeneous partial differential equation, which is related to this problem, is tackled by employing an exponential solution approach. After that, the evaluation of the boundary conditions results in a transcendental expression from which the buckling load and the corresponding buckling half-wave number can be obtained by means of numerical methods. A comparison between solutions for different orthotropic parameters, restraint stiffnesses, and load combinations reveals similarities of the solutions. Because of that, the solutions are approximated by simple functions via regression. Good agreement is found between regression functions and source data. Additionally, interaction curves for combined loadings are presented. By modification of the relation for compression–shear interaction in case of isotropic material, the application range can be extended to the case of an orthotropic plate strip with elastically restrained edges. Again, differences between the source data and the interaction formulations are observed to be very small.

Nomenclature

a	=	plate length, exponent of interaction formula
b	=	plate width
$\bar{a}$	=	affine plate length
$\bar{b}$	=	affine plate width
c_φ	=	spring constant
$\bar{c}_\varphi$	=	dimensionless spring constant
$[D]$	=	bending stiffness matrix
h_i, p_i, q_i	=	abbreviations in polynomial expressions
IK	=	interaction criterion
$[K]$	=	coefficient matrix
k_x, k_y, k_{xy}	=	buckling coefficients
$\bar{M}_y$	=	affine bending moment
m	=	number of buckling half-waves in longitudinal direction
N_x, N_y, N_{xy}	=	in-plane loads
R_x, R_{xy}	=	ratios of buckling coefficients
$\{W\}$	=	vector of deflection amplitudes
w	=	deflection normal to the plate
x, y, z	=	Cartesian coordinates
$\bar{x}$, $\bar{y}$, $\bar{z}$	=	affine Cartesian coordinates
$\bar{\alpha}$	=	modified aspect ratio
β_m	=	related half-wave number
δ_{ab}	=	ratio of loads
η	=	parameter of orthotropy
λ_n	=	roots of characteristic polynomial

Received 27 October 2010; accepted for publication 28 December 2010.

*Doctoral Candidate, Department of Aeronautical and Automotive Engineering, Berliner Tor 9; matthias.beerhorst@haw-hamburg.de.

†Professor, Department of Aeronautical and Automotive Engineering, Berliner Tor 9; michael.seibel@haw-hamburg.de.

‡Senior Engineer, Methods and Tools, Karnapp 25; christian.mittelstedt@airbus.com.

I. Introduction

APART from strength and stiffness the structural stability is an important aspect in the design of lightweight structures for aerospace vehicles. For the stability analysis in the predesign stage structural components as stiffened shells which can be found for example in the fuselage, wing or empennage structures are often decomposed into subcomponents. A typical representative of these subcomponents is the plate strip with elastically restrained edges, which can be used as a mechanical model for the web of a thin-walled profile or the skin between stiffeners (see Fig. 1a). The support which is provided by the adjacent subcomponents can be expressed through the stiffness of the rotational springs [1]. Because of the circumstance that with increasing modified aspect ratio the buckling load of the plate with finite length converges from above toward the buckling load of a plate strip the buckling analysis of the plate strip always delivers conservative results. Furthermore, the values of the buckling loads for these two plate types do only slightly differ if the modified aspect ratio exceeds three. Figure 1b visualizes the structural configuration which is treated in this study. The orthotropic plate strip is elastically restrained along its longitudinal edges by rotational springs and loaded by a combination of homogeneous uniaxial compression in the longitudinal direction and in-plane shear.

Investigations concerning the buckling of plate strips under combined loadings have been the subject of scientific research since many decades. A thorough survey of the work performed until 1970 may be found in [2]. The case of the isotropic plate strip under combined compression and in-plane shear with its longitudinal edges elastically restrained is for example examined in [3]. In this work the exact solution of the partial differential equation (PDE) is evaluated and additionally an approximate solution procedure based on an energy method is discussed. Dörfler [4] presents the exact solution for the case of an orthotropic laminate. In [5] an extension of the problem which includes a fully occupied matrix of bending stiffness is given. However, the boundary conditions discussed in this treatise are limited to the classical cases of simply supported and clamped edges. Extensive analysis results for the buckling loads of general, symmetric laminates with simply supported and clamped edges under compression, shear and in-plane bending are presented by

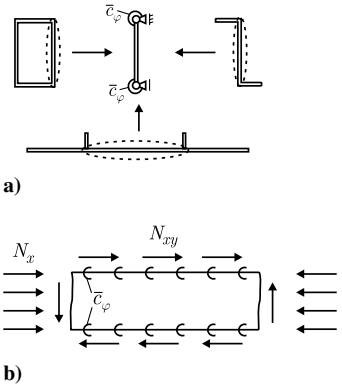

Fig. 1 Segmentation of structures into a) subcomponents and b) structural configuration.

Nemeth [6,7]. Herein, a calculation procedure based on an energy formulation in combination with the Rayleigh–Ritz method is applied. General information concerning the mechanics of composite plates can be found for example in [8–10].

The intention of the present paper is to produce diagrams of generic buckling curves by evaluation of the exact solution according to Dörfler [4]. These diagrams shall on the one hand reveal the influence of different parameters and on the other hand provide results in an easy to access manner which can be used in predesign. Furthermore, simple approximate formulas for the calculation of the buckling load are developed which can be readily integrated into predesign and optimization algorithms. The present method is limited to the case of symmetric orthotropic laminates because in the case of generally laminated composites the bending moments would not only be related to the out-of-plane deflections, but also to the in-plane displacements. Thus, for these quantities two extra solution approaches would be needed and the chance of obtaining an exact transcendent solution for the problem becomes very small. Additionally, the amount of different parameters that occur due to the coupling terms increases drastically, making a regression-based approximation approach become unsuitable. Most important, nearly all laminates that are used in aeronautical engineering consist of symmetric laminate layups. A comparison between the interaction formula for isotropic materials [11] and an enhanced interaction formula for orthotropic materials closes this investigation.

II. Governing Equations

According to the theory of linear statics equilibrium conditions the following PDE of fourth order describes the buckling of orthotropic plates [8]:

$$D_{11}\frac{\partial^4 w}{\partial x^4} + 2(D_{12}+2D_{66})\frac{\partial^4 w}{\partial x^2 \partial y^2} + D_{22}\frac{\partial^4 w}{\partial y^4} + N_x\frac{\partial^2 w}{\partial x^2} + N_y\frac{\partial^2 w}{\partial y^2} + 2N_{xy}\frac{\partial^2 w}{\partial x \partial y} = 0 \tag{1}$$

Herein, the elements of the bending stiffness matrix are denoted with D_{ij}, the external forces with N_{ab} and the deflection with w. Introduction of the subsequently following expressions will allow a nondimensional representation of Eq. (1). With Eq. (2) an implicit definition of the buckling coefficients k_{ab} is given:

$$N_x = k_x\left(\frac{\pi}{b}\right)^2\sqrt{D_{11}D_{22}} \qquad N_y = k_y\left(\frac{\pi}{b}\right)^2 D_{22}$$
$$N_{xy} = k_{xy}\left(\frac{\pi}{b}\right)^2\sqrt[4]{D_{11}D_{22}^3} \tag{2}$$

Furthermore, the following affine coordinates and dimensions are employed [12]:

$$x = \sqrt[4]{D_{11}}\bar{x} \qquad y = \sqrt[4]{D_{22}}\bar{y} \tag{3}$$

$$a = \sqrt[4]{D_{11}}\bar{a} \qquad b = \sqrt[4]{D_{22}}\bar{b} \tag{4}$$

For a plate of the length a and width b the modified aspect ratio can now be written as

$$\bar{\alpha} = \frac{\bar{a}}{\bar{b}} = \frac{a}{b}\sqrt[4]{\frac{D_{22}}{D_{11}}} \tag{5}$$

The related number of half-waves for a buckling mode with m half-waves then reads

$$\beta_m = \frac{m\pi}{\bar{\alpha}} \tag{6}$$

Moreover, the following parameter of orthotropy is applied:

$$\eta = \frac{D_{12}+2D_{66}}{\sqrt{D_{11}D_{22}}} \tag{7}$$

Hereby, PDE (1) can be transformed to

$$\frac{\partial^4 w}{\partial \bar{x}^4} + 2\eta\frac{\partial^4 w}{\partial \bar{x}^2 \partial \bar{y}^2} + \frac{\partial^4 w}{\partial \bar{y}^4} + k_x\left(\frac{\pi}{\bar{b}}\right)^2\frac{\partial^2 w}{\partial \bar{x}^2} + k_y\left(\frac{\pi}{\bar{b}}\right)^2\frac{\partial^2 w}{\partial \bar{y}^2} + 2k_{xy}\left(\frac{\pi}{\bar{b}}\right)^2\frac{\partial^2 w}{\partial \bar{x}\partial \bar{y}} = 0 \tag{8}$$

To solve the preceding equation an exponential approach, which is of periodic form in the longitudinal direction is employed:

$$w(\bar{x},\bar{y}) = W\underbrace{e^{i\left(\frac{m\pi\bar{x}}{\bar{a}}\right)}}_{w_1(\bar{x})}\underbrace{e^{i\lambda\frac{\bar{y}}{\bar{b}}}}_{w_2(\bar{y})} \tag{9}$$

Inserting Eq. (9) into Eq. (8) yields a quartic equation for λ:

$$\left(\frac{m\pi}{\bar{a}}\right)^4 + 2\eta\left(\frac{m\pi}{\bar{a}}\right)^2\left(\frac{\lambda}{\bar{b}}\right)^2 + \left(\frac{\lambda}{\bar{b}}\right)^4 - k_x\left(\frac{m\pi}{\bar{a}}\right)^2\left(\frac{\pi}{\bar{b}}\right)^2 - k_y\left(\frac{\pi}{\bar{b}}\right)^2\left(\frac{\lambda}{\bar{b}}\right)^2 - 2k_{xy}\left(\frac{\pi}{\bar{b}}\right)^2\left(\frac{m\pi}{\bar{a}}\right)\left(\frac{\lambda}{\bar{b}}\right) = 0 \tag{10}$$

The application of the related buckling half-wave number β_m according to Eq. (6) allows for a more compact and completely generic representation of this equation:

$$\lambda^4 + h_2\lambda^2 + h_1\lambda + h_0 = 0 \qquad h_2 = -k_y\pi^2 + 2\eta\beta_m^2$$
$$h_1 = -2k_{xy}\beta_m\pi^2 \qquad h_0 = -k_x\beta_m^2\pi^2 + \beta_m^4 \tag{11}$$

If the structure is not loaded by shear, the equation becomes biquadratic:

$$\lambda^4 + h_2\lambda^2 + h_0 = 0 \tag{12}$$

To reduce the number of unknowns concerning the buckling coefficients it is convenient to express them through related quantities. Because of this the ratio δ between the minor buckling coefficients and the dominant reference buckling coefficient is introduced:

$$\delta_{ab} = \frac{k_{ab}}{k_{\text{ref}}}, \qquad (a,b = x,y) \tag{13}$$

In Eq. (14) this is exemplary illustrated for the case of predominating longitudinal compression:

$$k_{\text{ref}} = k_x \Rightarrow \delta_x = 1, \qquad \delta_y = \frac{k_y}{k_x}, \qquad \delta_{xy} = \frac{k_{xy}}{k_x} \tag{14}$$

III. Boundary Conditions and Calculation of the Buckling Load

For the plate strip with elastically restrained longitudinal edges the deflection at the longitudinal edges has to vanish:

$$w(\bar{x},\bar{y}=0) = 0 \qquad w(\bar{x},\bar{y}=\bar{b}) = 0 \tag{15}$$

Besides, at this position the bending moment is proportional to the rotation:

$$\bar{M}_y(\bar{x},\bar{y}=0) = -\frac{\partial^2 w}{\partial \bar{y}^2}(\bar{x},\bar{y}=0) = -\frac{\bar{c}_\varphi}{\bar{b}}\frac{\partial w}{\partial \bar{y}}(\bar{x},\bar{y}=0)$$

$$\bar{M}_y(\bar{x},\bar{y}=\bar{b}) = -\frac{\partial^2 w}{\partial \bar{y}^2}(\bar{x},\bar{y}=\bar{b}) = \frac{\bar{c}_\varphi}{\bar{b}}\frac{\partial w}{\partial \bar{y}}(\bar{x},\bar{y}=\bar{b}) \tag{16}$$

Herein, the proportionality factor is the dimensionless spring constant $\bar{c}_\varphi$:

$$\bar{c}_\varphi = \frac{c_\varphi b}{D_{22}} \tag{17}$$

Inserting the approach of Eq. (9) into the boundary conditions (15) and (16) yields the following four homogeneous equations:

$$\sum_{n=1}^{4} W_n \underbrace{1}_{K_{1n}} = 0 \qquad \sum_{n=1}^{4} W_n \underbrace{e^{i\lambda_n}}_{K_{3n}} = 0$$

$$\sum_{n=1}^{4} W_n \underbrace{\lambda_n(\lambda_n + i\bar{c}_\varphi)}_{K_{2n}} = 0 \qquad \sum_{n=1}^{4} W_n \underbrace{e^{i\lambda_n}\lambda_n(\lambda_n - i\bar{c}_\varphi)}_{K_{4n}} = 0 \tag{18}$$

Herein, the $K_{kl}(k,l=1\ldots4)$ represent the elements of the coefficient matrix. Thus, Eq. (18) can be written in a more compact way as

$$[K]\{W\} = \{0\} \tag{19}$$

The necessary condition for a nontrivial solution of the system of equations is a vanishing determinant of the coefficient matrix:

$$|[K]| = 0 \tag{20}$$

In this expression the only unknowns that remain are the buckling coefficient k and the related half-wave number β_m. Because the transcendental nature of the preceding equation the solution can only be obtained by application of an iterative solution procedure. The combination of k and β_m, which fulfills Eq. (20) and simultaneously delivers a minimum value for k, represents the solution. In the present study β_m was varied employing the bisection method and the resulting nonlinear equation was solved for the remaining unknown k in each step.

IV. Results

A. Pure Compression

A graphical illustration of the solution for pure compressive loading is given in Fig. 2. It can be observed that the buckling load increases with increasing η. An increase of the spring stiffness also leads to a rise of the buckling load, herein the alteration is huge in the area of small $\bar{c}_\varphi$ and only insignificant for $\bar{c}_\varphi$ values of 50 and above. The shape of the curves is observed to be very similar. Figure 3 visualizes the related half-wave number for the case of pure compression. Here, the shape of the graphs is also similar and the alterations are the biggest in the area of small spring stiffnesses. Generally it can be observed that the related half-wave number increases with rising values of the spring stiffness and η. But the dependence on the orthotropy parameter η is significantly smaller than in the case of the buckling coefficient, for small values of $\bar{c}_\varphi$ even negligible.

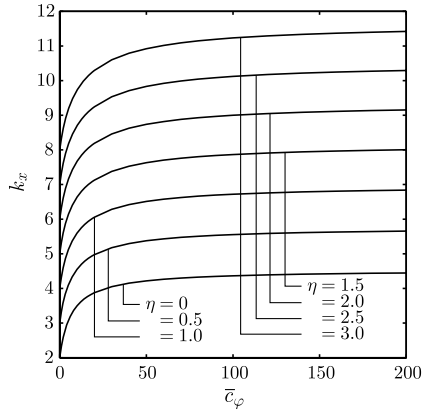

Fig. 2 Buckling coefficient for pure compression depending on $\bar{c}_\varphi$ and η.

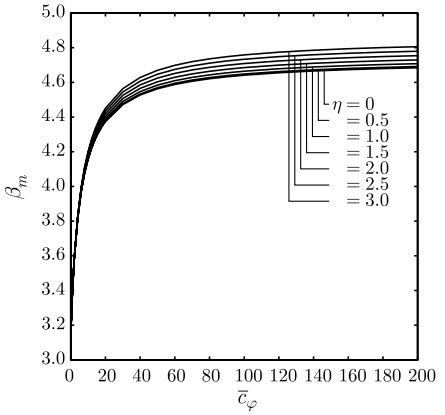

Fig. 3 Related half-wave number for pure compression depending on $\bar{c}_\varphi$ and η.

B. Pure Shear

Regarding the influencing variables η and $\bar{c}_\varphi$ the buckling factor behaves similar as in the case of pure compression (see Figs. 4 and 5). So the relations discussed for pure compression are also valid in the case of pure shear loading. However, the shapes of the curves showing the related half-wave number are considerably different (Fig. 5). For a constant value of η these curves look more like the graphs of the buckling coefficient shown in Figs. 2 and 4, but controversially the related half-wave number decreases with increasing η. The influence of η and $\bar{c}_\varphi$ on the buckling factor and related half-wave number for combined loadings can be found in the Appendix (Figs. A1–A3). Herein, the variable δ according to Eq. (13) expresses the ratio of the two buckling factors.

V. Approximate Solutions for Buckling Coefficient and Related Half-Wave Number

Although the algorithm as prescribed in Sec. III allows for the determination of the buckling coefficient and the related half-wave number, for application areas such as predesign and optimization it is more convenient to employ approximate solutions which are of vastly higher computational efficiency. Bearing in mind the knowledge gained in Sec. IV regarding the general dependency of buckling coefficient and related half-wave number on spring stiffness and orthotropy parameter in the following regression-based approximate functions for these two quantities will be derived. For this purpose a

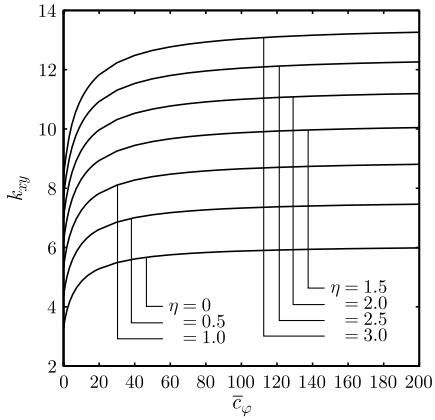

Fig. 4 Buckling coefficient for pure shear depending on $\bar{c}_\varphi$ and η.

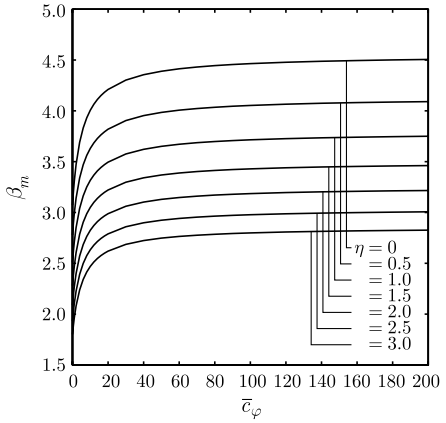

Fig. 5 Related half-wave number for pure shear depending on $\bar{c}_\varphi$ and η.

comprehensive amount of data for the buckling coefficient and the related half-wave number is generated. More precisely, all possible combinations of 31-η- and 56-$\bar{c}_\varphi$ values, which makes a total of 1736 evaluation points, are taken into consideration. The interval of the η values ranges from 0 to 3 with steps of 0.1, that of the $\bar{c}_\varphi$ values from 0 to 1E12. In the latter case the step width is variable and increases with increasing $\bar{c}_\varphi$. If a surface is lain through the data points the intersection curves with a plane between one ordinate and the abscissa at different positions of η and $\bar{c}_\varphi$ look similar. For example the graphs in Fig. 2 can be interpreted as intersection curves between the surface of k_x over η and $\bar{c}_\varphi$ and a plane normal to the η axis at different η positions. Because of this circumstance it seems appropriate to divide the regression procedure into two successive regressions. In the first step at each η position an approach is made for the dependence on the spring constant for a constant η. Tests of different approaches revealed that a rational polynomial as given in Eq. (21) represents a good choice in this case:

$$f(\bar{c}_\varphi, \eta) = \frac{p_1 \cdot \bar{c}_\varphi + p_2}{\bar{c}_\varphi + q_1} \tag{21}$$

Herein, the coefficients p_i and q_i depend on η. In the second step a regression for these coefficients as a function of η will be performed.

A. Pure Compression

For the case of pure compression the coefficients p_i and q_i from Eq. (21) are provided for the buckling coefficient (22) and related half-wave number (23):

$$p_1(\eta) = 2.326\eta + 4.584 \qquad p_2(\eta) = 2.52\eta^2 + 19.15\eta + 13.95$$
$$q_1(\eta) = \frac{28.65\eta + 75.35}{\eta + 10.77} \tag{22}$$

$$p_1(\eta) = 0.007\eta^2 + 0.023\eta + 4.72$$
$$p_2(\eta) = \frac{0.864\eta + 18.02\eta + 44.4}{\eta + 2.468}$$
$$q_1(\eta) = \frac{0.272\eta + 5.71\eta + 13.63}{\eta + 2.39} \tag{23}$$

B. Pure Shear

If the structure is loaded solely by shear the following expressions can be used to approximate the buckling coefficient (24) and related half-wave number (25):

$$p_1(\eta) = \frac{41.65\eta + 69.73}{\eta + 11.42} \qquad p_2(\eta) = \frac{234\eta + 220.7}{\eta + 8.13}$$
$$q_1(\eta) = \frac{10.44\eta + 8.83}{\eta + 1.08} \tag{24}$$

$$p_1(\eta) = \frac{22.9}{\eta + 5.04} \qquad p_2(\eta) = 0.457\eta^2 - 4\eta + 18.35$$
$$q_1(\eta) = 0.0115\eta^5 - 0.109\eta^4 + 0.3916\eta^3 - 0.621\eta^2 + 0.3\eta + 5.914 \tag{25}$$

The bandwidth of the relative deviation between the solution of the PDE and the values obtained from the regression functions is summarized in Table 1. Since it is always smaller than 2.5% the results obtained from the regression functions are quite reliable.

VI. Interaction Formula for Combined Compression–Shear Loading

In the case of combined loads it is usual to depict the results in the form of interaction curves. The coordinates of a point in the diagram are determined by the ratio R between the current load to the maximum allowable load for the specific type of load of Eq. (26):

$$R_x = \frac{k_x}{k_{x,\max}}; \qquad R_{xy} = \frac{k_{xy}}{k_{xy,\max}} \tag{26}$$

In the first instance the characteristics of the interaction curves for the current structure and loading conditions shall be examined. For this purpose it is helpful to consider the dependency of the curve path R_x over R_{xy} regarding $\bar{c}_\varphi$ and η in a separate manner. Figures 6 and 7 visualize a situation in which the spring constant is kept constant and η is varied. The case of $\eta = 1$ corresponds to an isotropic plate strip. It can be observed that in both figures the curves are moving outwards with increasing η. A rising spring constant has the consequence that the distance between the curves increases slightly.

In Figs. 8 and 9 interaction curves with constant η and a variable spring stiffness are shown. It can be readily observed that the influence of the spring stiffness is very small because the curves in Figs. 8 and 9 are nearly congruent.

In contrast to the both figures discussed before the sequence of the curves now changes from the inside to the outside. For $\eta = 0$ the curves show the tendency to move outward with decreasing spring stiffness, whereas in the case of $\eta = 3$ it is just the other way round. The limit case in which the sequence of the curves changes from inward to outward lies at $\eta = 1$. Here, all curves for arbitrarily spring stiffnesses are congruent.

The purpose of the current examination is to investigate if the application range of the interaction formula which is valid for isotropic materials can be extended in a way that it is also applicable for an orthotropic plate strip with elastically restrained longitudinal edges. For isotropic materials the interaction formula reads

$$R_x + R_{xy}^2 = 1 \tag{27}$$

Herein, R denotes the ratio of loads according to Eq. (26). In a survey of the buckling of isotropic and orthotropic plates [2] a work [13] is cited which states that the interaction formula (27) could also be used for orthotropic plates. Unfortunately the cited work was not accessible to the authors of the current work and thus the facts which lead to the preceding proposal could not be reconstructed.

However, at this point a more general approach for the interaction formula is made:

$$R_x + R_{xy}^a = 1 \tag{28}$$

As foundation for the following considerations the load ratios according to Eq. (26) are calculated for a number of $\eta - \bar{c}_\varphi$

Table 1 Maximum and minimum relative deviation between regression solutions and solutions of the PDE

	Δ, %			
Loading	k		β_m	
Pure compression	−2.5	−0.1	−0.5	0.5
Pure shear	−1.9	−0.1	−1.0	1.0

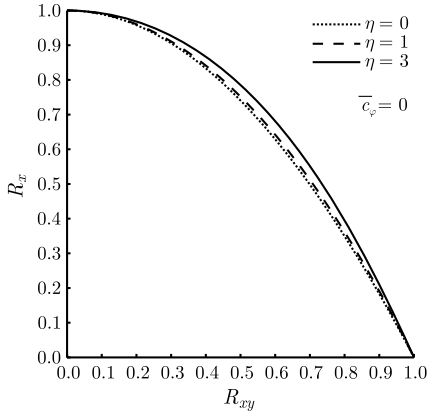

Fig. 6 Interaction curves for $\bar{c}_\varphi = 0$ and variable η.

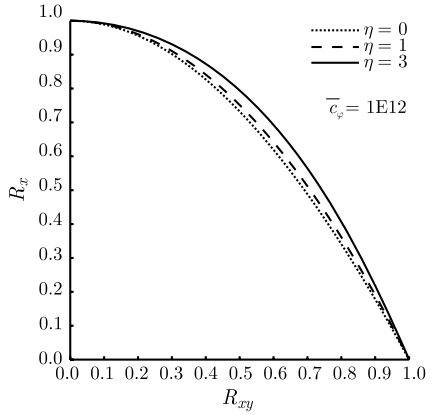

Fig. 7 Interaction curves for $\bar{c}_\varphi = 1E12$ and variable η.

combinations. The η values range from 0 to 3 in steps of 0.2, whereas $\bar{c}_\varphi$ takes the values 0, 2, 4, 8, 20, 200, 1000 and 1E12. Additionally the ratio δ according to Eq. (13) is varied inside the spectrum from pure compression to pure shear with an increment of 0.0125. This leads to a total of 20,608 values which shall secure that the presented results are valid for the complete bandwidth of load ratios, orthotropy parameters and spring stiffnesses.

From the evaluation of the interaction curves two essential aspects regarding the influence of the parameters $\bar{c}_\varphi$ and η shall be taken into consideration when developing a general interaction formula:

1) As it can be seen from Figs. 6 and 7 the sensitivity of the curves concerning η are relatively distinctive and should not be disregarded.

2) The nearly congruent curves in Figs. 8 and 9 indicate that the influence of the spring stiffness is very small. Therefore, the spring constant will not be considered for the determination of the exponent a from Eq. (28).

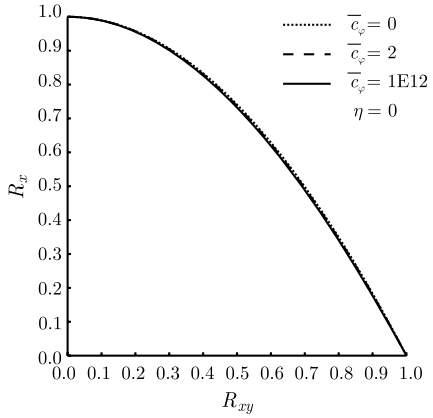

Fig. 8 Interaction curves for $\eta = 0$ and variable $\bar{c}_\varphi$.

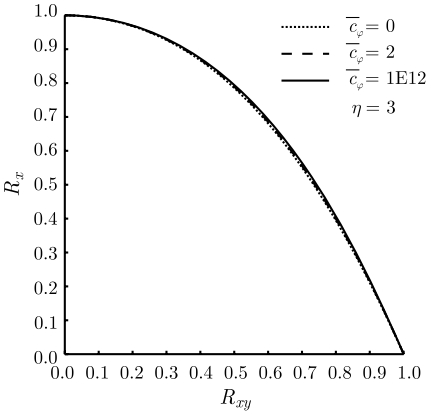

Fig. 9 Interaction curves for $\eta = 3$ and variable $\bar{c}_\varphi$.

The intention to cover the whole bandwidth of $\eta - \bar{c}_\varphi$ combinations with the new general interaction formula and the associated amount of data led to the decision to automate the regression procedure using a script. In this procedure miscellaneous types of functions as well as different degrees are employed. A polynomial of second order turns out to be the best compromise between complexity and accuracy in Eq. (29):

$$a = 0.007\eta^2 + 0.1\eta + 1.9 \tag{29}$$

In the case of an isotropic material η amounts to 1, leading to a value of 2.007 for a which is only negligibly different from $a = 2$ according to Eq. (27).

In the following a short explanation on the determination of the reserve factor is given. Illustrations are provided in Fig. 10. To calculate the reserve factor for a certain loading situation which is represented by the point P the distance p between the origin and the point P with the coordinates R_{xy} and R_x is needed. Additionally the length of the segment r which lies on the same line of application as p and connects the origin with the interaction curve has to be taken into account. The reserve factor can now be calculated as

$$\mathrm{RF} = \frac{r}{p} \tag{30}$$

If an approximation is applied to describe the interaction curve as depicted in Fig. 10 the relative deviation reads

$$\Delta = \frac{r_2 - r_1}{r_1} \tag{31}$$

When the enhanced expression is used as exponent, the spectrum of relative deviation only lies between −0.73 to 0.68% (see Table 2). For comparison Table 2 also shows the error spectrum which has to be accepted if the interaction formula (27) is applied which was originally developed for isotropic materials.

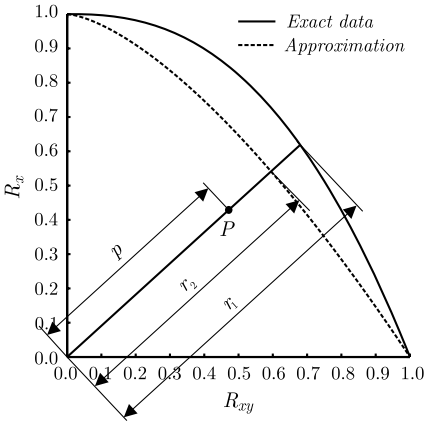

Fig. 10 Interaction diagram including essential segments for the determination of the reserve factor.

Table 2 Maximum and minimum relative deviation between interaction curves and solutions of the PDE

Interaction criterion	Δ, %	
IK_{new}	−0.73	0.68
IK_{iso}	−3.77	1.56

VII. Conclusions

The illustration of the solution of the PDE of the discussed problem in form of generic curves provides a good insight into the buckling behavior of the plate strip loaded by combined compression and in-plane shear. Because of the similarity of the curve shapes regression formulas can be obtained which allow for an approximation of the results of the PDE with an accuracy of 3% while demanding considerably lower computational effort.

Using the extended interaction formula derived in this work the actual path of the interaction curve can be described notably better than by using the formula which is known from the isotropic case. Because of this, the bandwidth of the relative error can be reduced from about 5.5 to less than 1.5%.

The regression formula for the buckling load as well as the one for the interaction curves may be advantageously applied in areas where under acceptance of a certain deviation especially the low computational effort is of decisive importance. This is often the case in the fields of optimization and preliminary design.

To the authors' knowledge, no test results for the buckling of long flat orthotropic plates under combined loading are available in open literature. Because of this, the validation of the presented theory with test results remains the subject of future investigations.

Appendix: Generic Diagrams of Buckling Factors and Related Half-Wave Numbers

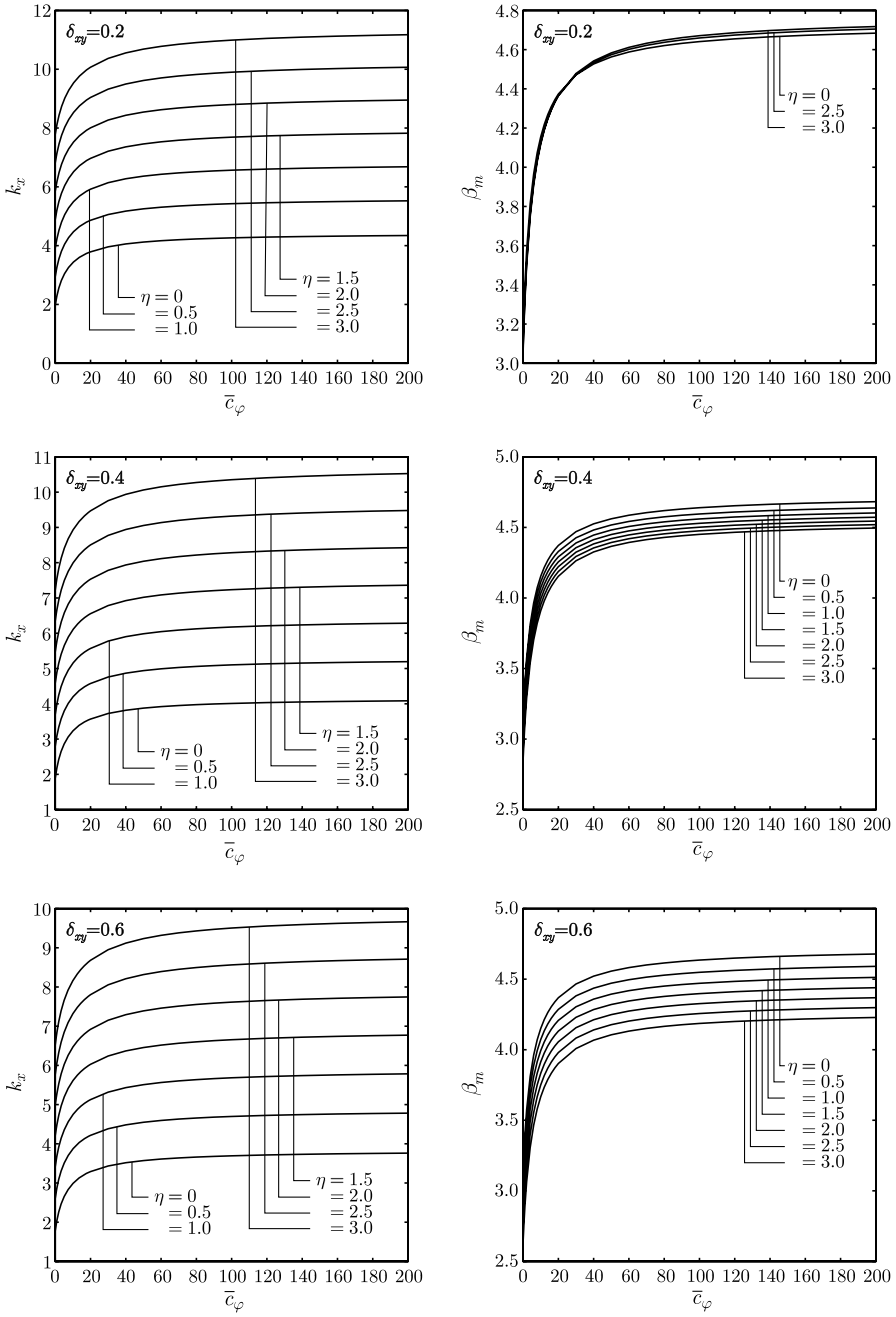

Fig. A1 Buckling factors and related half-wave numbers, part 1.

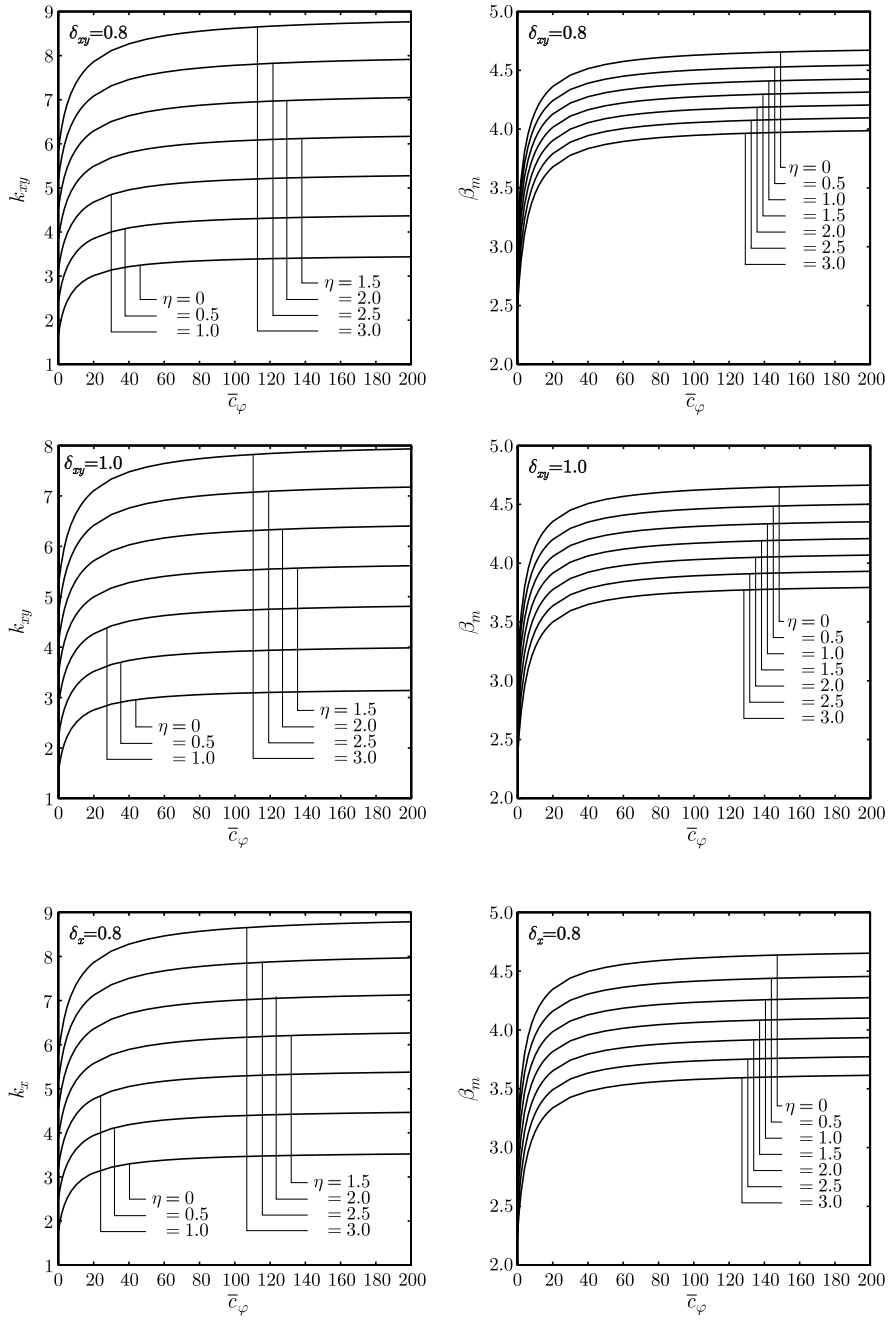

Fig. A2 Buckling factors and related half-wave numbers, part 2.

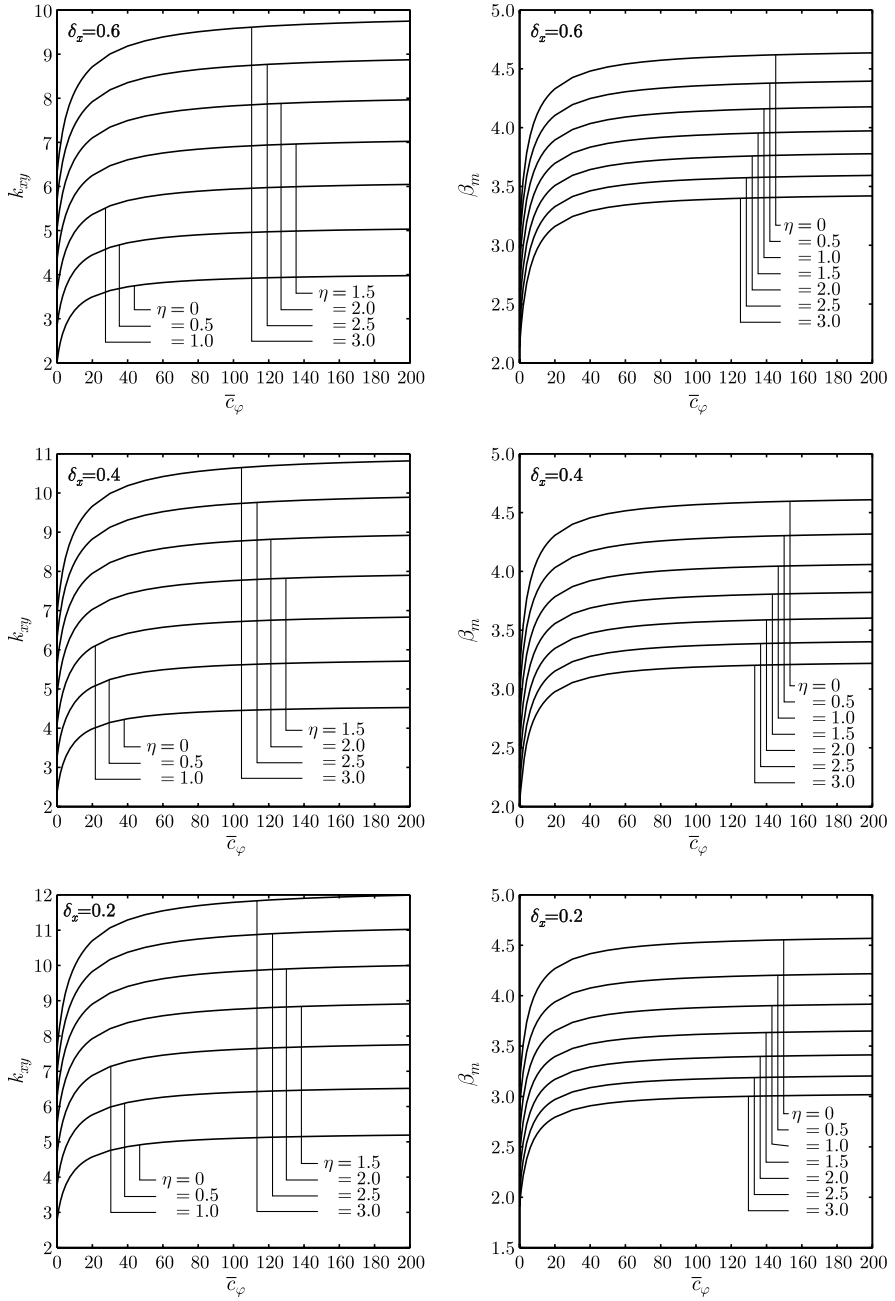

Fig. A3 Buckling factors and related half-wave numbers, part 3.

References

[1] Qiao, P., Davalos, J. F., and Wang, J., "Local Buckling of Composite FRP Shapes by Discrete Plate Analysis," *Journal of Structural Engineering*, Vol. 127, No. 3, 2001, pp. 245–255. doi:10.1061/(ASCE)0733-9445(2001)127:3(245)

[2] Johns, D. J., "Shear Buckling of Isotropic and Orthotropic Plates: A Review," Ministry of Defense TR 3677, London, 1971.

[3] Stowell, E. Z., and Schwartz, E. B., "Critical Stress for an Infinitely Long Flat Plate with Elastically Restrained Edges Under Combined Shear and Direct Stress," NACA Rept. ARR 3K13, Hampton, VA, 1943.

[4] Dörfler, T., *Beulverhalten und Optimierung längsversteifter Gurtplatten unter Schub- und Druckbelastung*, Vol. 229, Fortschritts-Berichte VDI Reihe 1, VDI-Verlag, Düsseldorf, Germany, 1993.

[5] Thielemann, W., "Contribution to the Problem of Buckling of Orthotropic Plates, with Special Reference to Plywood," NACA TM 1263, Hampton, VA, 1950.

[6] Nemeth, M. P., "Buckling Behavior of Long Symmetrically Laminated Plates Subjected to Combined Loadings," NASA TP 3195, Hampton, VA, 1992.

[7] Nemeth, M. P., "Buckling Behavior of Long Anisotropic Plates Subjected to Combined Loads," NASA TP 3568, Hampton, VA, 1995.

[8] Jones, R. M., *Mechanics of Composite Materials*, 2nd ed., Taylor and Francis, Philadelphia, 1999.

[9] Kollar, L. P., and Springer, G. S., *Mechanics of Composite Structures*, Cambridge Univ. Press, Cambridge, England, U.K., 2003.

[10] Wiedemann, J., et al., *Leichtbau: Elemente und Konstruktion*, 3rd ed., Klassiker der Technik, Springer, Berlin, 2007.

[11] Shanley, F. R., *Strength of Materials*, McGraw–Hill, New York, 1957.

[12] Brunelle, E. J., and Oyibo, G. A., "Generic Buckling Curves for Specially Orthotropic Rectangular Plates," *AIAA Journal*, Vol. 21, No. 8, 1982, pp. 1150–1156.

[13] Buckling of Orthotropic Plates (Corrugated Plate Applications)," Bell Aerosystems, Rept. 7-60-941001, 1961.